STRUCTURE OF THE KOREAN PENINSULA FROM WAVEFORM TRAVEL-TIME ANALYSIS

Roland Gritto[1], Jacob E. Siegel[1], and Winston W. Chan[2]

Array Information Technology[1] and Harris Corporation[2]

Sponsored by Air Force Research Laboratory

Contract No. FA8718-06-C0006

ABSTRACT

Seismic waveform data of the Korean Meteorological Administration (KMA) have been analyzed to perform 3-D tomographic travel-time inversions to produce high-resolution 3-D crustal P- and S-wave velocity models for the South Korean peninsula. In a first step, waveform data from 2001 through May 2008 have been analyzed to map the Moho discontinuity below South Korea using refracted Pn travel times. Phase-arrival information from both velocity and accelerometer sensors was collected. The analysis included 270 events throughout the region producing 8,860 phase picks of Pg, Pn, Sg/Lg, and Sn phases. A total of 5,090 P-wave and 3,770 S-wave phases were identified. Using the combination of all available velocity and accelerometer data from the 119 KMA stations, it was possible to estimate depth locations for 226 KMA events. The hypocenters were subsequently used to derive travel-time distance curves based on 1-D velocity models to appraise the quality of the travel-time picks. The analysis produced, respectively, crustal P- and S-wave velocities of 6.13 km/s and 3.57 km/s and upper mantle velocities of 8.02 km/s and 4.48 km/s. The travel-time distance curves were used to determine static corrections for all station locations. After applying static corrections to all observed travel-times, refracted P-wave phases along the Moho boundary were selected from the dataset to estimate the depth and topography of the Moho discontinuity beneath South Korea. The resulting Moho topography reveals a relatively flat interface with depth variations from 28 to 34 km. The shallowest parts are below the Yellow Sea and below the Sea of Japan, while the deepest structure is located below the Yeongnam Massif. Joint inversion for hypocenters and velocity structure was performed to derive 3-D P- and S-wave velocity models for the crust. The inversion was constrained by the depth of the Moho interface derived in the previous step. Using analyst phase picks, it was possible to reduce the variance between observed and calculated travel times by 77%. Compared to preliminary event locations based on the 1-D velocity model, the relocated events indicate crustal seismicity deeper than 20 km beneath the peninsula. Additionally, a gradual decrease in depth of seismicity is observed beneath the Yellow Sea. The obtained 3-D velocity distribution is not correlated with the geologic terrains of the peninsula. The velocity distribution is relatively homogeneous corroborating the good fit of the 1-D velocity model. Upper crust velocity values are estimated at 6.2 km/s and 3.6 km/s for P- and S-waves respectively. These values increase beneath 25 km to 7 km/s for P- and 4.3 km/s for S-waves. Mantle velocities are encountered below 32 km depth reaching 8.5 km/s and 4.8 km/s for P- and S-waves, respectively, corroborating the results of the Moho topography study. Finally, 35 GT5 events were selected from the 270 relocated events using Bondár's criteria (Bondár et al., 2004). The 35 events are well located within the dense KMA network as required by Bondár's criteria.

Report Documentation Page

Form Approved
OMB No. 0704-0188

1. REPORT DATE	2. REPORT TYPE	3. DATES COVERED
SEP 2008		**00-00-2008 to 00-00-2008**

4. TITLE AND SUBTITLE	5a. CONTRACT NUMBER
Structure of the Korean Peninsula from Waveform Travel-Time Analysis	5b. GRANT NUMBER
	5c. PROGRAM ELEMENT NUMBER
6. AUTHOR(S)	5d. PROJECT NUMBER
	5e. TASK NUMBER
	5f. WORK UNIT NUMBER
7. PERFORMING ORGANIZATION NAME(S) AND ADDRESS(ES) **Array Information Technology,140 Bessemaur Dr,East Lansing,MI,48823**	8. PERFORMING ORGANIZATION REPORT NUMBER
9. SPONSORING/MONITORING AGENCY NAME(S) AND ADDRESS(ES)	10. SPONSOR/MONITOR'S ACRONYM(S)
	11. SPONSOR/MONITOR'S REPORT NUMBER(S)

12. DISTRIBUTION/AVAILABILITY STATEMENT
Approved for public release; distribution unlimited

13. SUPPLEMENTARY NOTES
Proceedings of the 30th Monitoring Research Review: Ground-Based Nuclear Explosion Monitoring Technologies, 23-25 Sep 2008, Portsmouth, VA sponsored by the National Nuclear Security Administration (NNSA) and the Air Force Research Laboratory (AFRL)

14. ABSTRACT
see report

15. SUBJECT TERMS

16. SECURITY CLASSIFICATION OF:			17. LIMITATION OF ABSTRACT	18. NUMBER OF PAGES	19a. NAME OF RESPONSIBLE PERSON
a. REPORT **unclassified**	b. ABSTRACT **unclassified**	c. THIS PAGE **unclassified**	**Same as Report (SAR)**	**12**	

OBJECTIVES

The primary objective of this research is to produce high-resolution 3-Dcrustal P- and S-wave velocity models of the South Korean Peninsula. The structure of the crustal model will be supplemented by the derivation of a 3-D Moho interface below the peninsula. The resulting velocity and structural models will provide valuable information for regionalization and relocation studies.

RESEARCH ACCOMPLISHED

Waveform data from the Korean Meteorological Administration (KMA) were analyzed for the years 2001 through May 2008 to determine the phase arrival of body waves from local and regional events. The KMA operates a dense seismic network consisting of 138 stations with velocity and accelerometer sensors. The analyzed data consist of triggered waveforms recorded for local and regional events throughout the Korean Peninsula. Phase arrival information of P- and S-waves was subsequently used to delineate the structure of the Moho interface between crust and mantle.

Korean Meteorological Administration (KMA) Waveform Data

The KMA of the Republic of Korea (ROK) operates a dense network of seismic stations throughout the country. The network consists of 138 stations comprised of velocity and accelerometer sensors. Station configurations include combinations of velocity and accelerometer sensors as well as single sensor sites. The analyzed data included triggered waveforms of local and regional events from 2001 through May 2008. For stations with single sensor configuration, the analyzed data were obtained from either velocity or accelerometer data, while both velocity and accelerometer data were obtained for those stations with dual sensor configuration. The intention is to improve the significance of data for stations where travel-time data from more than one instrument are available.

Travel-Time Analysis of KMA Waveform Data

The analysis of the KMA waveform data produced a total of 8,860 phase picks from 270 events located throughout the Korean Peninsula. The number of located events amounts to a seismicity rate of approximately 32 events per year and confirms previous estimates for this region. Identified phases included Pg, Pn, Sg/Lg, and Sn. The number of individual identified phases amounted to 5,090 P-wave and 3,770 S-wave phases. Because the accelerometer data contain higher frequency information, epicentral distances from the events to the accelerometer stations were generally shorter than those associated with velocity stations, which helped to constrain the depth of the events. Furthermore, this approach decreased the uncertainty of the hypocenter location. Using the combination of velocity and accelerometer data, it was possible to estimate depth locations for 230 of the KMA events.

Quality control of the data was performed using travel-time-distance curves. The phase picks of the KMA data from January 2001 – May 2008 are shown in Figure 1. The travel-time of P- and S-wave phases is plotted as a function of hypocentral distance to assess the quality of the selected phase picks. The diamond-shaped symbols represent the P- and S-wave phases determined from the waveform data. The short black horizontal lines at each data point represent the relative location error for each hypocenter estimate associated with that phase pick. For each hypocenter, a relative error is calculated separately for the x-, y- and z-direction. In order to facilitate the presentation of this uncertainty, we take the relative errors for the three directions and calculate a single resulting vector, which represents the radius of a sphere around each hypocenter estimate indicating the uncertainty in its location. Therefore, the short black horizontal lines in Figure 1 represent the length of the radius of the error sphere for each hypocenter estimate. In contrast, the short black vertical lines at each data point represent the relative timing error for the event time associated with that phase pick. Considering all phase picks from velocity and accelerometer data, the average hypocentral error was reduced by 17% relative to the original hypocenters published by the KMA. The colored solid lines in Figure 1 represent the best linear fit, in a least-squares sense, through the cloud of travel-time picks. It can be seen that the fit is very good for hypocentral distances below 400 km. Although the number of events decreases for hypocentral distances beyond 400 km, the linear fit is still good at greater distances. The velocity values listed in Figure 1 are averaged P- and S-wave velocities of the crust and upper mantel as determined from the slope of the travel-time distance curves. These values are in good agreement with published estimates for the Korean Peninsula (i.e., Chang and Baag, 2006). If the model of a single-layered crust is employed to determine average crustal thickness from the travel-time curves in Figure 1, a value of 32 km is obtained. In comparison, Chang and Baag (2006) conducted receiver function studies based on teleseismic body wave data. They report a distribution of crustal thicknesses from 28 km in the eastern part to 35

km in the south-western part of South Korea. Therefore, the average value of 32 km, determined from the phase picks of the KMA data, appears to be a good estimate for crustal thickness, giving confidence in the obtained arrival times. A separate method to estimate Moho topography is presented below.

KMA GT5 Events

GT events are important benchmarks to test earthquake location techniques and validate velocity models. We applied Bondár's criteria (Bondár et al., 2004) to the database of 230 KMA events with depth locations requiring that each potential GT5 event is located:

(a) by at least 10 stations, all within 250 km distance from the epicenter;
(b) with an azimuth gap of less than 110^o;
(c) with a secondary azimuth gap of less than160^o; and
(d) by at least one stations within 30 km distance from the epicenter.

Forty-four events were identified that matched these criteria, each one having a cumulative location error δe of less than 5 km. The cumulative location error is defined as:

$$\delta e = \sqrt{\delta x^2 + \delta y^2 + \delta z^2}$$

where δx, δy, and δz are location errors in longitude, latitude and depth, respectively. Figure 2 shows GT5 events identified from the KMA hypocenter database. They are well located within the dense network of KMA stations as required by Bondár's criteria.

Estimation of 3-D Moho Structure from Refracted P-waves

Two important parameters that define crustal structure are the depth and topography of the Moho boundary between crust and mantle. The topography of this interface can help to explain crustal tectonics and consequently the kinematics of wave propagation through the crust. Refracted P-wave phases along the Moho boundary can be used to estimate the depth of this interface. As can be seen in Figure 1, refracted Pn phases were observed between hypocentral distances from 130 km to 650 km. In total, 810 Pn phases were collected from the KMA data from January 2001–May 2008.

Before the depth and topography of the Moho could be estimated, near-station effects due to inhomogeneities in the near subsurface had to be removed from the Pn travel times. These static corrections prevent travel-time anomalies from near surface inhomogeneities to be mapped into anomalies of Moho elevation at depth. The static corrections were estimated using a least-squares approach minimizing the misfit between observed and calculated Pg travel times. The least-squares approach jointly inverted for a homogenous crustal velocity model and static correction terms at each recording station. These static corrections were subsequently subtracted from the Pn travel times before they were used to estimate Moho topography.

Several approximations have to be considered when estimating depth from travel times of refracted waves. The most important is that of a one-dimensional velocity model of a layer over a half space. In the current case, the velocity estimates for the crust and upper mantle derived from the linear fits in Figure 1 are utilized. Furthermore, it is assumed that the Moho interface is piece-wise flat over the propagation distance of each refracted phase along this boundary, while dip of the flat segments is allowed. A sketch indicating the geometric assumptions is presented in Figure 3. With these approximations, ray theory and the principles of refraction seismology were applied to determine Moho depth and topography. For each refracted ray path, two depth-estimates for the Moho interface below the hypocenter and recording station were calculated together with the dip of the Moho interface between these two points. A maximum-likelihood approach was applied to the results of a grid search over a two dimensional depth-and-dip space to minimize the misfit between observed and calculated Pn travel times. Once the depth and dip of the Moho interface was determined below each hypocenter and recording station, the data were interpolated using an adjustable-tension continuous-curvature surface-gridding approach (Wessel and Smith, 1995). The result of the gridding is shown in Figure 4, which displays a 3-D surface plot of the Moho interface below South Korea. The emerging pattern reveals a slightly undulating interface with a mean depth of 31 km. The Moho appears elevated extending from the north-east through the center to the south-west at a depth of approximately 29 km. To the north and south of this structure, the interface dips down to about 34 km, while it

appears to be elevated below the Yellow Sea and the Sea of Japan. The mean depth of the Moho interface will be used to constrain the inversion for 3-D velocity structure presented in the next section.

Three-Dimensional Crustal Velocity Structure

The number of phase picks obtained from waveform analysis between January 2001 and May 2008 amounted to 8,400. However, not all of these phase picks can be utilized during the velocity inversion as the implemented ray tracing is based on the eikonal solver by Podvin and Lecomte (1991), which considers first arrivals only. Therefore, Pg- and Sg-phases will only be considered for distances shorter than their respective crossover distances, while Pn- and Sn phases will be used beyond these distances. The ray density of all P-wave phases is presented in Figure 5, where it is superimposed on the Korean peninsula. The green circles and blue triangles denote, respectively, the epicenters of the events and the locations of the seismic stations. The red circles represent the node spacing implemented during the inversion.

The P-wave velocity estimates resulting from travel-time tomography produced homogeneous values of about 6 km/s for the upper crust, which suggest that these measurements cannot be used to differentiate the geologic terrains (refer to Figure 6). Below 25 km depth, the velocity increases to typical lower-crust values of about 7 km/s. At a 32-km depth, the transition from crustal- to mantle velocities can be observed. Variations in velocity range from 6.5 to 8.5 km/s, with the latter representing upper mantle velocities. The pattern of high- and low-velocity regions at 32 km depth correlates to some degree to the pattern of the Moho topography in Figure 3. The brown color in Figure 4 represents an elevated Moho, which indicates the presence of mantle material and thus higher velocities (blue color in Figure 6). In contrast, the blue color in Figure 4 represents a depressed Moho, which indicates the presence of crustal material and thus lower velocities (green colors in Figure 6).

The S-wave velocity estimates, presented in Figure 7, corroborate the results of the P-wave inversion to a certain degree. The velocity distribution is relatively smooth in the upper crust with values of 3.5 km/s. Variations in velocity, which could indicate the presence of different geologic terrains, are not apparent. The velocity values appear to decrease in the lower part of the crust. However, this may be an artifact caused by the poor ray coverage at this depth range, due to the lack of sufficient Sn phase arrivals at longer distances.

CONCLUSIONS AND RECOMMENDATIONS

To interpret the Moho topography, it is necessary to incorporate the crustal tectonics of the Korean Peninsula. Although the pattern of Moho topography reveals a northeast/southwest trend, a correlation to the general trend of the major geologic terrains of the Korean Peninsula is only weakly developed. Nevertheless, the Moho coincides to a certain degree with surface topography. The central depression of the Moho interface is co-located with the Yeongnam Massif, which may indicate isostatic compensation for this mountain range (Kwon and Yang, 1985; Choi and Shin, 1996). This feature is common in most investigations of crustal structure in this region.

Analysis of phase information derived from KMA waveform data points to a relatively homogenous crust below South Korea. The good linear fit through the travel-time distance data in Figure 1, as well as the homogenous velocity distribution obtained from 3-D velocity inversions indicates crustal structure with little variation with respect to seismic velocities. Therefore, the geologic terrains, observed at the surface cannot be separated by seismic velocities at depth. The results derived in this study for the Moho topography are corroborated by the work of Chang and Baag (2006) and Yoo et al. (2007), who mapped the Moho interface using surface-wave dispersion and receiver-function analyses. In both studies, a pattern of the Moho interface, similar to the one displayed in Figures 3 was found. The fact that the results of our refraction study, which was based on a 1-D velocity model, match the results of these previous studies, indicate that a 1-D velocity model is an acceptable approximation, at least for the upper half of the crust below South Korea.

ACKNOWLEDGEMENTS

The figures and maps throughout this document were created using the Generic Mapping Tools by Wessel and Smith (1995).

REFERENCES

Bondár, I., S.C. Myers, E. R. Engdahl and E.A. Bergman (2004). Epicenter accuracy based on seismic network criteria, *Geophys. J. Int* 156: 483–496.

Chang, S. J. and C. E. Baag (2006). Crustal Structure in South Korea from Joint Analysis of Broadband Waveforms and Travel Times, *Bull. Seis. Soc. Am*. 96: 856–870, doi:10.1785/0120040165.

Choi, K. S. and Y. H. Shin (1996). Isostasy in and around the Korean Peninsula by analyzing gravity and topography data, *J. Geol. Soc. Korea* 32: 407–420.

Kwon, B. D. and S. Y. Yang (1985). A study on the crustal structure of the southern Korean Peninsula through gravity analysis, *J. Korean Inst. Mining Geol*. 18: 309–320.

Podvin, P. and I. Lecomte (1991). Finite difference computation of travel times in very contrasted velocity models: A massively parallel approach and its associated tools, *Geophys. J. In*t. 105: 271–284.

Wessel, P. and Smith, W. (1995). New version of the generic mapping tools released. *EOS Trans. AGU* 76: 329.

Yoo, H. J., R. B. Herrmann, K. H. Cho, and K. Lee (2007). Imaging the three-dimensional crust of the Korean Peninsula by joint inversion of surface-wave dispersion and teleseismic receiver functions, *Bull. Seism. Am.* 97: 3, 1002–1011, doi: 10.1785/0120060134.

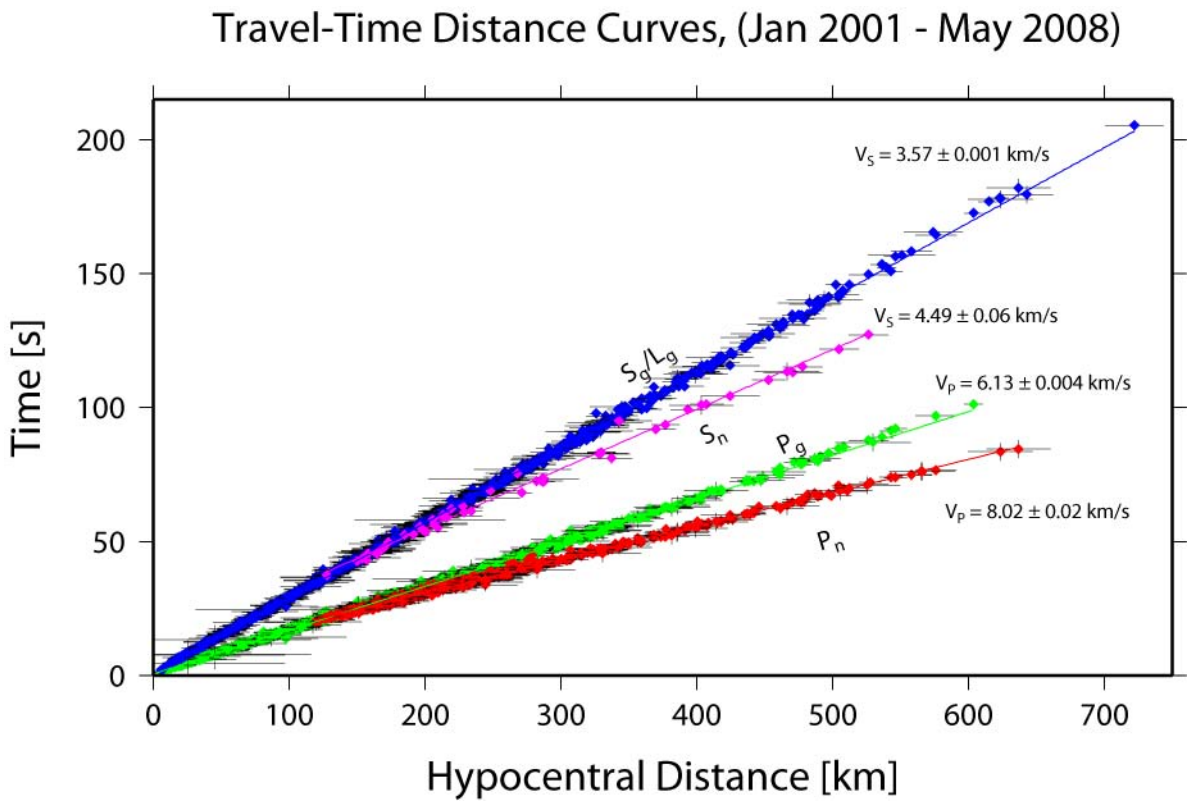

Figure 1. Travel time as a function of hypocentral distance for the P- and S-wave phase picks as determined from KMA waveform data for the period January 2001- May 2008. The phase picks are indicated by colored diamonds, while the solid colored lines represent their best least-squares fit resulting in the velocity values as noted. The short black horizontal lines at each data point represent the relative location error for each hypocenter estimate associated with that phase pick. The short black vertical lines at each data point represent the relative timing error for event time associated with that phase pick.

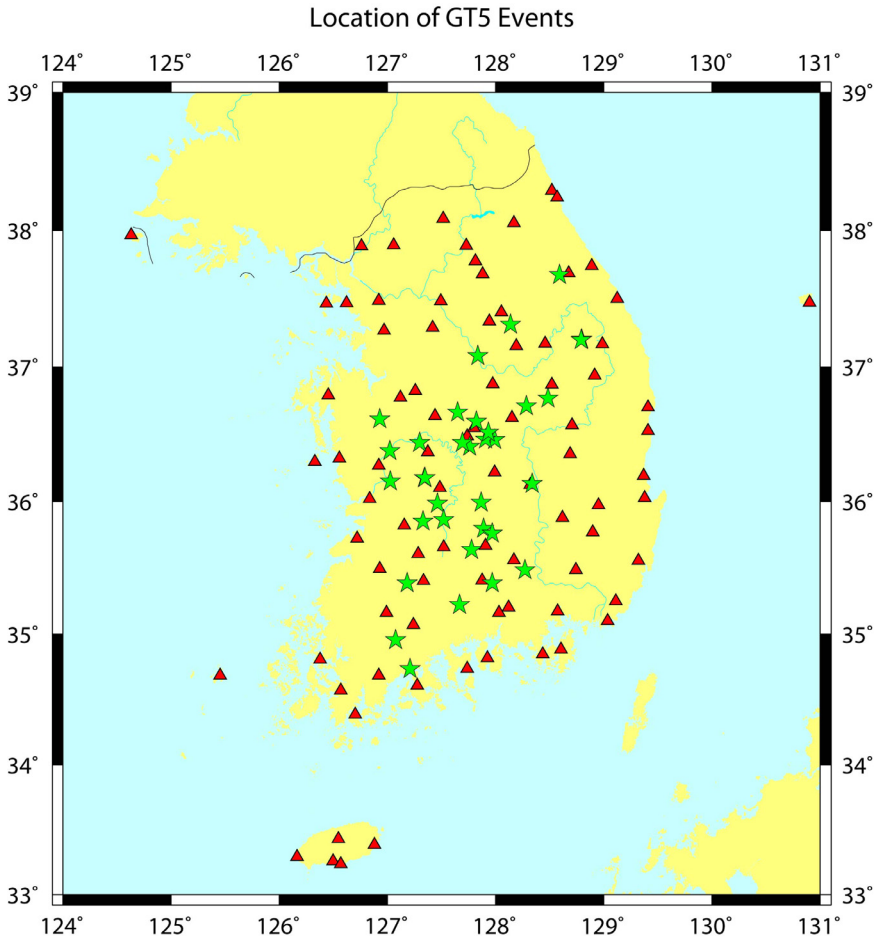

Figure 2. GT5 events identified from a database of 230 events with depth location derived from KMA waveform data from January 2001 – May 2008. Green starts denote epicenter of GT5 events, while the red triangles represent the KMA stations.

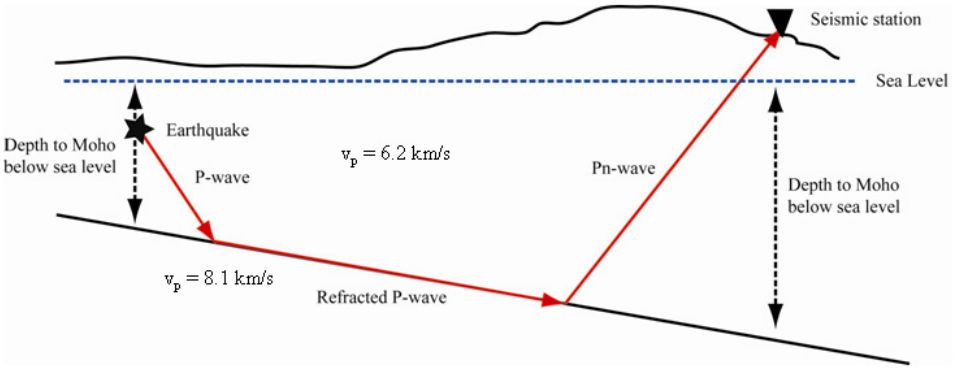

Figure 3. Sketch indicating the geometry for calculating theoretical travel times for refracted waves.

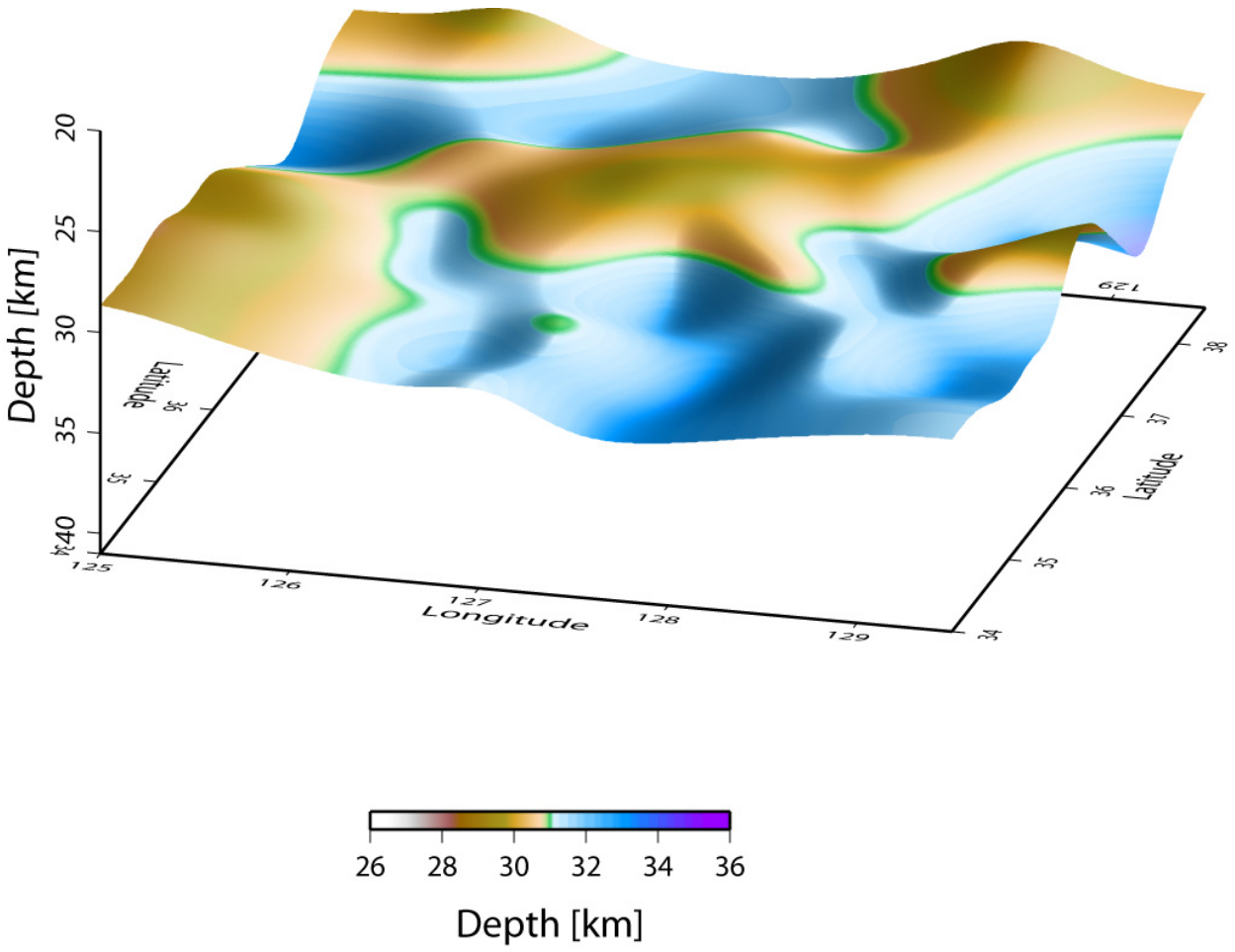

Figure 4. Three-dimensional surface plot of the Moho discontinuity below South Korea based on depth estimates below each KMA station and each recorded earthquake.

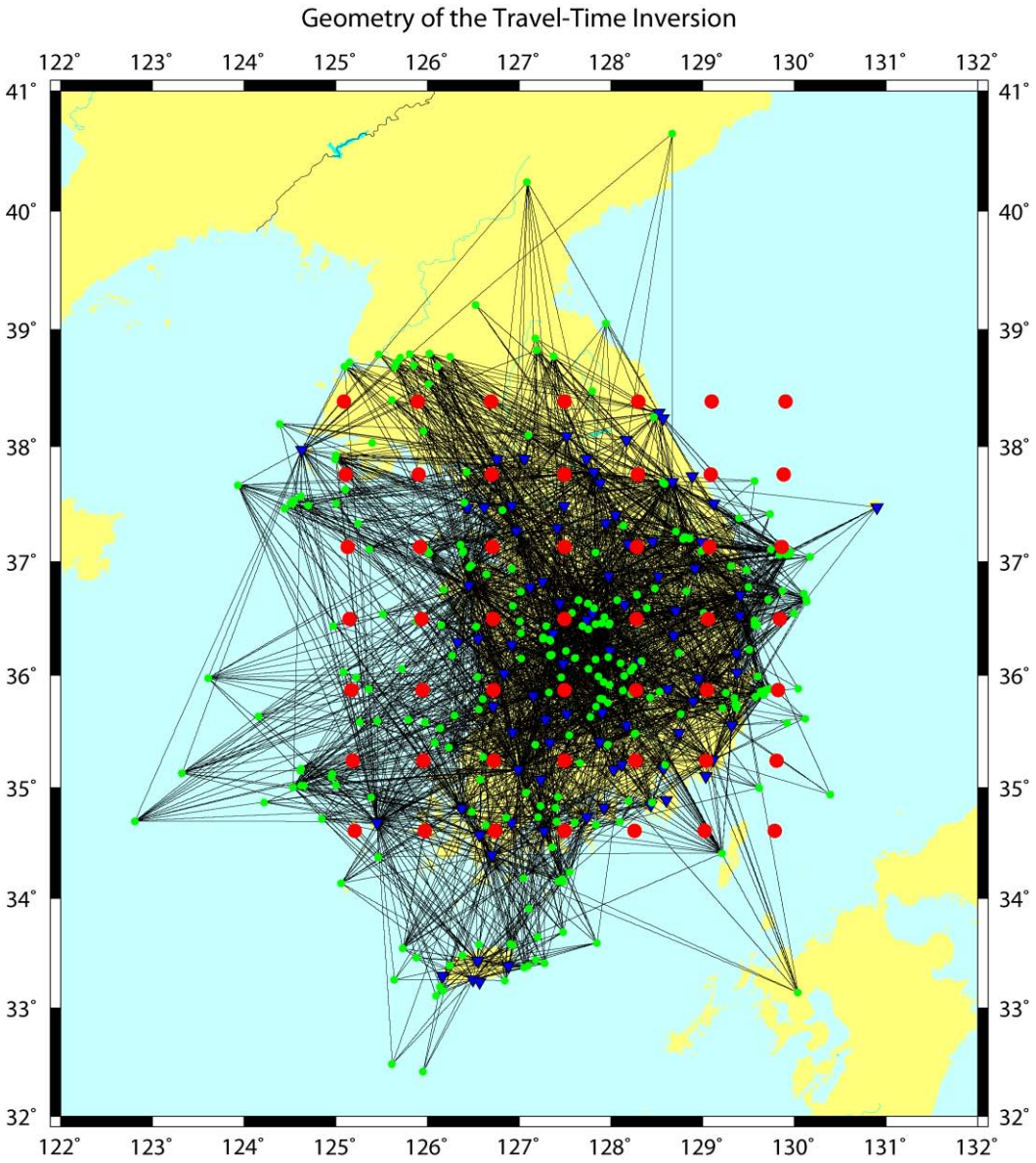

Figure 5. Geometry of the inverse problem. The P-wave (Pg and Pn) ray density is projected onto the surface, while the red circles indicate the nodes used during the inversion. Green circles and blue triangles indicate epicenters and seismic stations, respectively.

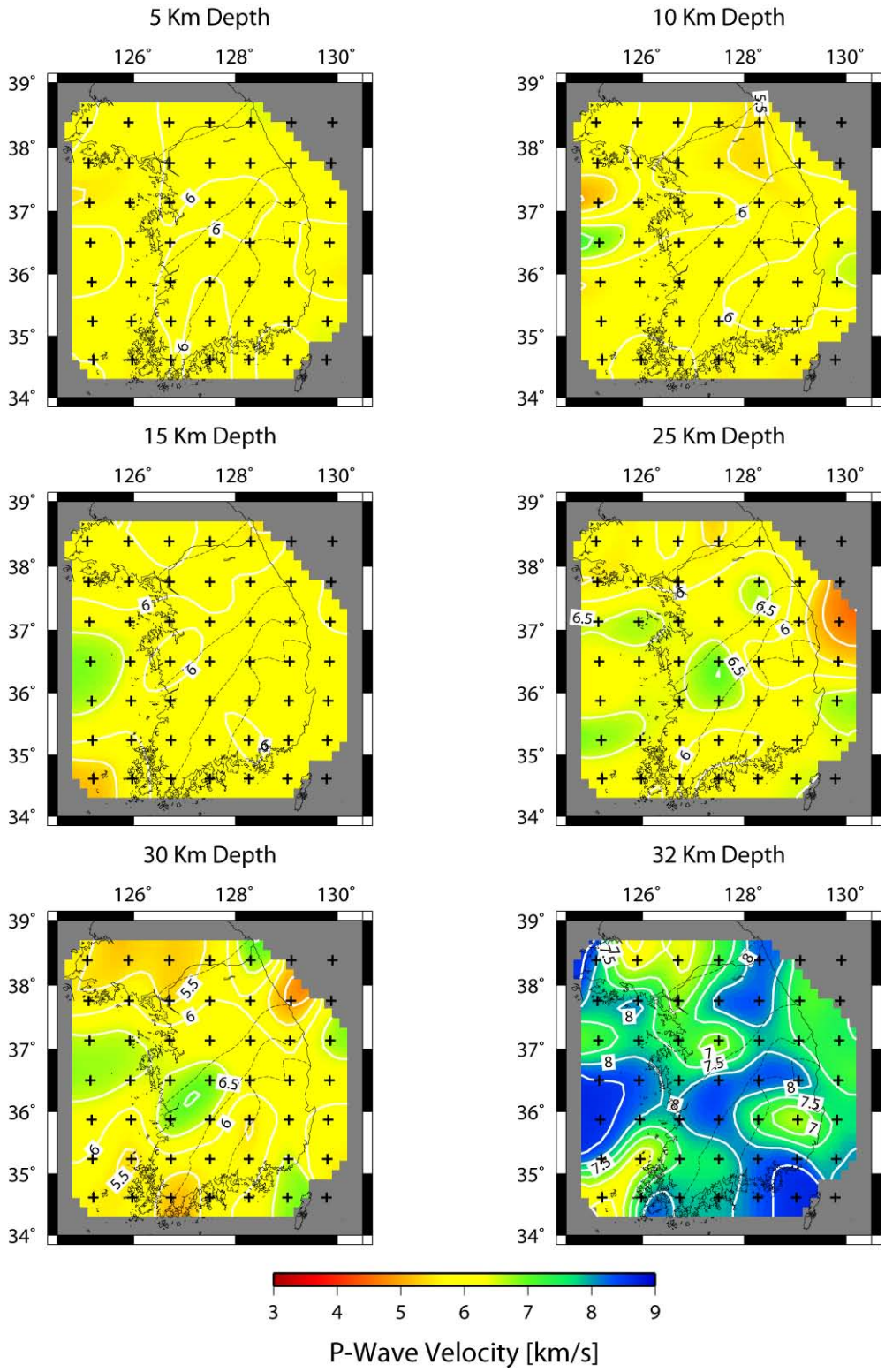

Figure 6. Horizontal cross-sections of P-wave velocity distribution as a function of depth derived from 3,315 Pg and Pn phases and 270 earthquakes distributed across South Korea.

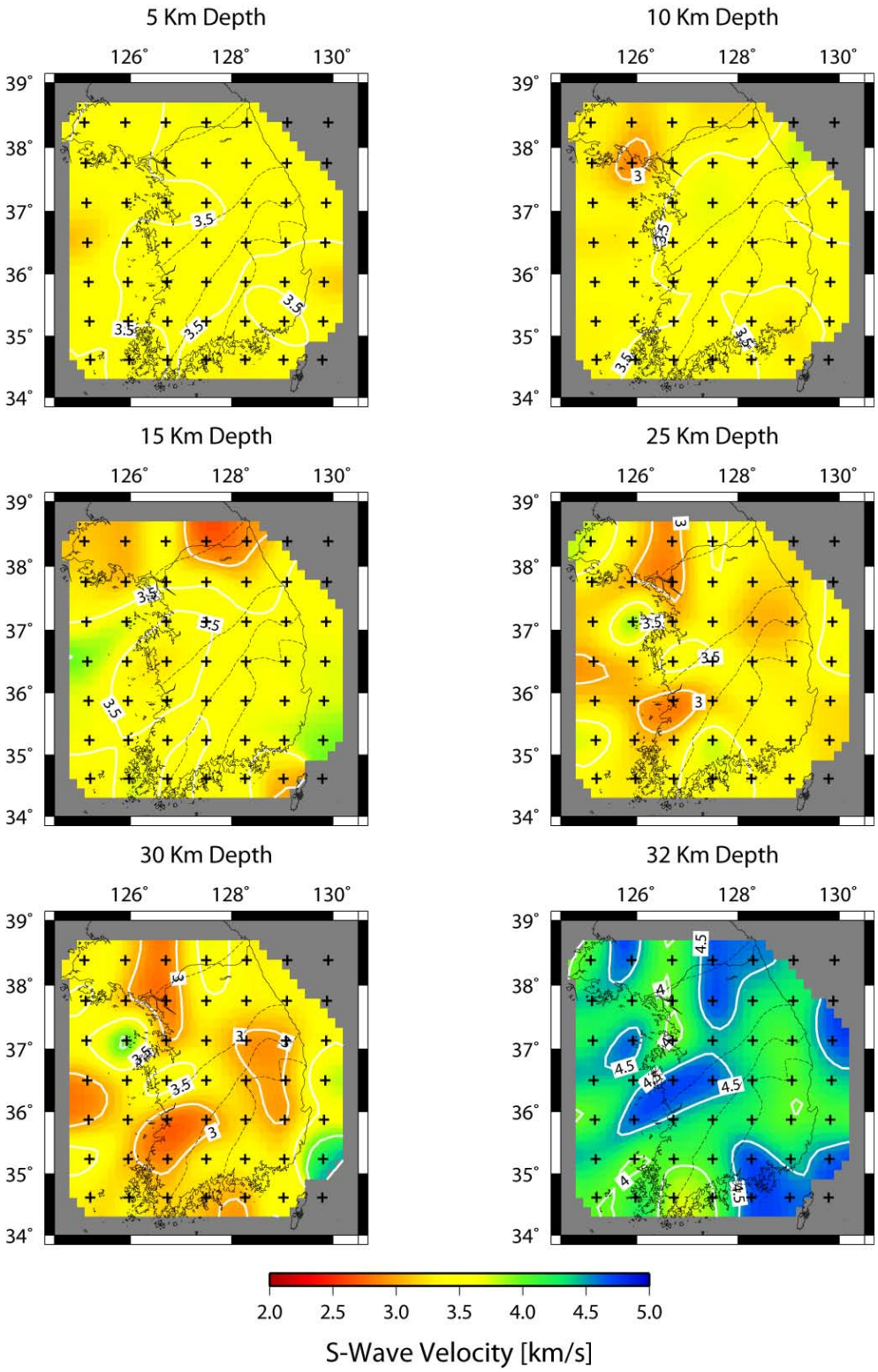

Figure 7. Horizontal cross-sections of S-wave velocity distribution as a function of depth derived from 2,279 Sg and Sn phases and 270 earthquakes distributed across South Korea.